Astron. Astrophys. 355, 915–921 (2000)

ASTRONOMY AND ASTROPHYSICS

Precession, beaming and the periodic light curve of OJ287

Z. Abraham

Instituto Astronômico e Geofísico, Universidade de São Paulo, São Paulo, Brazil

Received 29 November 1999 / Accepted 17 January 2000

Abstract. The strong periodic optical flares of OJ287 are explained in terms of the increase in the beaming factor when a precessing jet approaches the line of sight. The geometrical parameters of the precession are determined from the kinematical properties of the parsec scale superluminal features in the radio jet. The possible values of the Lorentz factor γ for the bulk motion in the jet are constrained by the half-life of the optical flares. A moderate value, $\gamma \approx 7$, gives the best fitting to the data.

Key words: galaxies: BL Lacertae objects: individual: OJ287 – galaxies: jets – radio continuum: galaxies – galaxies: magnetic fields – galaxies: photometry

1. Introduction

OJ287 is a BL Lac object which presents violent optical variability. Its light curve, going back to almost 100 years, shows three different types of variability. The strongest flares, of more than three magnitudes in the V band have a duration of a few months, almost constant color indices and very similar temporal behavior (Sillanpää et al. 1985). They occur with a periodicity of about 11.6 years and a total of 8 consecutive maxima were already detected (Sillanpää et al. 1988, 1996). Variations of several months were observed in the recurrence period, and of two magnitudes in the flare intensity. Another type of variability is represented by non-periodic flares of smaller amplitude and duration of a few days. Their spectral evolution resemble synchrotron flares from expanding, initialy compact and optically thick regions (Kidger et al. 1991). Finally, low intensity flickering is continuously present, sometimes with very short time periodicity (Carrasco et al. 1985; González-Pérez et al. 1996). At radio frequencies, good correlation is found between variability at high frequencies and the occurrence of optical synchrotron flares, with very little or no delay between them. However, the very strong periodic optical flares do not seem to have counterparts in the radio region (Valtaoja 1996). A detailed study of variability at radio frequencies was made by Hughes et al. (1998) using wavelet analysis. They found a periodicity of 1.6 years in the complete data series and of 1.1 years close to the epoch of the 1983 optical flare.

OJ287 is highly polarized, both at optical and radio wavelengths. The degree of linear polarization and its position angle change with time scales of hours to years. The optical polarization appears to increase with decreasing flux densities, reaching values as high as 40% (Hagen-Thorn 1980; Smith et al. 1987; Sillanpää 1991). At radio frequencies the polarization of the total flux was never larger than 15% but individual VLBI features presented values of more than 64% (Roberts et al. 1987; Aller et al. 1991), imposing serious constraints to the beaming models (Cawthorne & Wardle 1988). A systematic change in the mean polarization angle was observed between 1971 and 1991, both at radio and at optical wavelengths, the dispersion around the mean value being larger at optical than at radio wavelengths (Sillanpää 1991).

OJ287 has also been detected at high energies. The X-ray flux densities varied by a factor of three between measurements spaced by several years. Upper limits obtained by HEAO 1 and ROSAT instruments increase this factor to 20 or more (Worral et al. 1982; Comastri et al. 1995; Urry et al. 1996). The γ-ray emission was below the detection limit of the CGRO/EGRET instrument, except for a marginal detection at the epoch of the 1994-1995 optical flare (Schrader et al. 1996).

At parsec scales OJ287 has a very compact structure and it is frequently used as a VLBI phase reference. As many other BL Lac objects, it presents a one-sided jet, even though extending for only 3 mas when observed at 5 and 8.4 GHz, with a few knots expanding at moderate superluminal velocities (Gabuzda et al. 1989; Gabuzda & Cawthorne 1996; Vicente et al. 1996). However, closely spaced 43 GHz VLBI observations at the epoch of the 1994 optical flare showed a large number of features, extending up to distances of 2 mas from the core, expanding with large superluminal velocities (Marscher & Marchenko 1997). Similar results were obtained in the analysis of Geodetic 8.3 GHz VLBI maps at epochs 1990-1996 (Tateyama et al. 1999). VLA images show radio structure at a distance of 25 arc sec from the core ($\sim$ 90 kpc). Very high dynamical maps reveal an underlying curved tail joining both sources (Kollgaard et al. 1992; Perlman & Stocke 1994). This extended structure was studied at optical wavelengths, both with ground based telescopes (Silanpää et al. 1999; Heidt et al. 1999) and the HST

Send offprint requests to: Z. Abraham

(Jannuzi et al. 1997). The more reliable ground base observations (NOT and VLT) show a compact host galaxy which has a small offset to the south with respect to the active nucleus. Several models involving a binary pair of black holes have been proposed to explain the observed optical periodicity. Models in which the optical variability period coincides with the orbital period were proposed by Sillanpää et al. (1988) and Lehto & Valtonen (1996). The optical flares would be produced by the interaction between the secondary, in a very eccentric orbit, and the accretion disk surrounding the primary black hole. Katz (1997) suggested an alternative model, also based in a pair of black holes, the flares would be due to the increase in the beaming factor when a precessing jet passes very near the line of sight. The precession would be driven by the gravitational torque of the companion on the accretion disk of the primary black hole. A similar model was used by Abraham & Carrara (1998) and Abraham & Romero (1999) to explain the variation of the superluminal velocities and position angles of the VLBI features in the jets of 3C279 and 3C273.

In this paper the model is applied to OJ287. Although the parsec scale structure and the kinematics of the superluminal features do not define the jet as well as in 3C273 or 3C279, the reliably determined optical period and the good temporal coverage of the light curve during the last strong flares compensate this deficiency. It was possible to obtain the geometrical parameters of the precessing jet and its Lorentz factor.

2. The precessing jet

Let us consider a relativistic jet, with a bulk velocity β, precessing with constant velocity ω and period T around an axis which forms an angle ϕ_0 with the line of sight and having a projected angle η_0 in the plane of the sky. The instantaneous position of the jet is represented by the angles ϕ and η and the aperture angle of the precessing cone is defined as Ω. The variation of these angles with the time t', measured in the frame fixed at the central source, can be expressed as (Abraham & Romero 1999):

$$\eta(t') = \arctan \frac{y}{x} \tag{1}$$

$$\phi(t') = \arcsin\,[(x^2+y^2)]^{1/2} \tag{2}$$

with

$$x = (\cos\Omega\sin\phi_0 + \sin\Omega\cos\phi_0\sin\omega t')\cos\eta_0 - \\ -\sin\Omega\cos\omega t'\sin\eta_0 \tag{3}$$

$$y = (\cos\Omega\sin\phi_0 + \sin\Omega\cos\phi_0\sin\omega t')\sin\eta_0 + \\ +\sin\Omega\cos\omega t'\cos\eta_0 \tag{4}$$

The viewing angle ϕ is not directly observable but it is related to the superluminal velocity of the components by:

$$\beta_{\rm obs} = \frac{\beta\sin\phi}{1-\beta\cos\phi} \tag{5}$$

Table 1. Properties of the VLBI jet in OJ287

Comp.	$\beta_{\rm obs}h$	η (deg)	t_0 (years)
K1	2.8 ± 0.4	-100 ± 10	1969.5 ± 1
K2	2.6 ± 0.4	-120 ± 10	1978.7 ± 1
K3	3.2 ± 0.4	-150 ± 10	1983.3 ± 1

The elapsed time between two events in the observer and source frames (Δt and $\Delta t'$ respectively) are related by the Doppler factor δ as:

$$\Delta t' = \delta(\phi,\gamma)\Delta t \tag{6}$$

with

$$\delta(\phi,\gamma) = \gamma^{-1}(1-\beta\cos\phi)^{-1} \tag{7}$$

and

$$\gamma = (1-\beta^2)^{-1/2} \tag{8}$$

The precession period was defined in the observer frame as 11.6 years, the mean spacing between the major optical flares (Sillanpää et al. 1988). The phase of the precessing jet was adjusted in such a way that the epoch of minimum approach to the line of sight coincided with the 1994.85 optical flare.

2.1. The geometrical parameters

The geometric and kinematic properties of superluminal features in the jet were used to determine the other parameters of the model. It was assumed that each feature moves out ballistically in a straight trajectory with constant speed. In this case, the position and viewing angles of each feature represent the corresponding angles of the jet at the epoch at which the feature was formed. The observed velocities $\beta_{\rm obs}$ depend, not only on the viewing angle and on the bulk velocity of the jet, but also on the cosmological parameters used to convert the observed proper motion μ into linear velocity:

$$\beta_{\rm obs} = \frac{q_0 z + (q_0-1)\left[(1+2q_0 z)^{\frac{1}{2}}-1\right]}{100 h {q_0}^2(1+z)}\mu \tag{9}$$

where $h = H_0/100$, H_0 is the Hubble constant in units of km s^{-1} Mpc^{-1}, q_0 the deceleration parameter and z the redshift ($z = 0.306$).

The velocities, position angles and epoch of formation of the superluminal components in the OJ287 jet were obtained from VLBI measurements at 6 and 3.6 cm (Roberts et al. 1987, Gabuzda et al. 1989, Gabuzda & Cawthorne 1996) and are listed in Table 1. The superluminal velocities were calculated for $h = 1$ and $q_0 = 0.5$. Only three features (named K1, K2 and K3) have observations in more than one epoch (3, 4 and 2 epochs, respectively), their position angles differ by as much as 50° but their velocities are similar, imposing restrictions on the possible models. Features K1 and K2, for which more than two

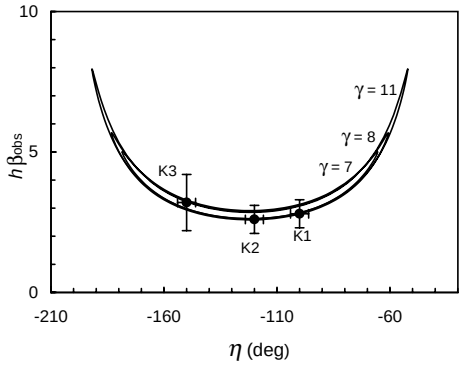

Fig. 1. Superluminal velocities $h\beta_{\rm obs}$ as a function of the position angle in the plane of the sky η for several combination of the parameters Ω, ϕ_0 and η_0 which fit the data points (K1, K2 and K3) for $\gamma = 7, 8$ and 11. The numbers near the curves represent the value of the corresponding parameter γ

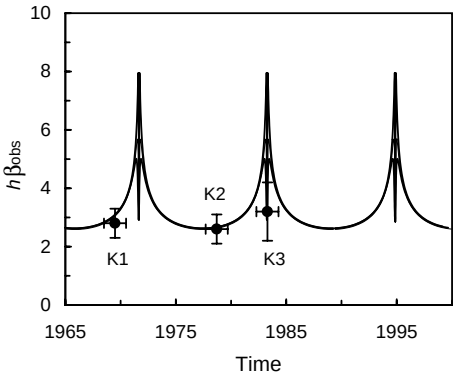

Fig. 2. Superluminal velocities $h\beta_{\rm obs}$ as a function of time in the observers reference frame for the combination of parameters presented in Fig. 1

Table 2. Parameters of the precessing model

γ	Ω (deg)	ϕ_0 (deg)	η_0 (deg)
7	12.8 ± 0.6	15.4 ± 1.0	-122 ± 5
8	13.6 ± 0.3	15.6 ± 0.4	-122 ± 6
11	14.3 ± 0.1	15.3 ± 0.1	-122 ± 6

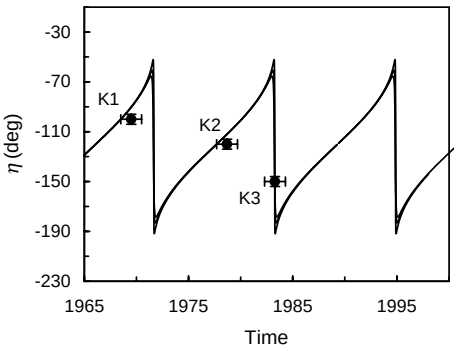

Fig. 3. Position angle in the plane of the sky η as a function of time in the observers reference frame for the combination of parameters presented in Fig. 1

epochs are available, show constant velocity, compatible with the assumption of ballistic motion. The position angles are more difficult to determine due to the poor north-south resolution. For this reason we attributed to them error bars that represent the variation of the reported values at different epochs instead of the smaller errors obtained from the model fitting programs. K1 and K2 were formed at the intervals between two major flares and their small velocities can be explained by large angles between the jet and the line of sight. K3, on the other hand, was formed around 1983.3, very close to the epoch of a large optical flare, when this angle was presumably small. These facts limit considerably the parameter space (Ω, ϕ_0, η_0) in which, for a given Lorentz factor, it is possible to obtain a good agreement between the model and the observations. We did not use the 43 GHz data of Marscher & Marchenko (1997) because only the distances to the core are available for the superluminal features, and also because their identification in the different maps is ambiguous, even though the observations were separated by only a few months. We used our model, instead, to interpret the data, as discussed in Sect. 2.4.

Fig. 1 shows the fitting, in the ($h\beta_{\rm obs}$, η)-space, for $h = 0.7$, of three models with $\gamma = 7$, 8 and 11 respectively. The parameters which define the models are listed in Table 2. The minimum value of the Lorentz factor for which a model could be fitted is $\gamma \approx 6$. Figs. 2 and 3 show that the solutions also fit the data in the $(h\beta_{\rm obs}, t)$ and (η, t)-space.

A different value of the Hubble constant will change the parameters of the precessing jet which fit the VLBI data and the optical light curve. A decrease in H_0 results in larger superluminal velocities and, as a consequence, larger values for γ. The fitting also shows that the amplitude of the precessing angle Ω and the viewing angle ϕ_0 decrease with h.

It is interesting to note that, although the features used in the fitting have moderate superluminal velocities, the larger velocities reported by Marscher & Marchenko (1997) are predicted by the models. In fact, as the jet approaches the line of sight, the observed velocity increases up to its maximum value, $\gamma(1-\gamma^{-2})^{1/2}$, and then decreases again as the viewing angle continuous to decrease. The Doppler factor, on the other hand, increases continuously and reaches its maximum value when the jet forms its smallest angle with the line of sight. In this position the beaming of the radiation can originate the optical flares, as will be discussed in the next section. It can also be observed that the position angles of the features found by Tateyama et al. (1999) change from $-110°$ (C1, C2, C3) to about $-90°$ (C6), also in agreement with the present model. The reported velocities, however, are much larger at all epochs. The reason could be the reduced number of features allowed in the model fitting, as can be seen when they are compared to the numerous 43 GHz features detected by Marscher & Marchenko (1997) at similar epochs.

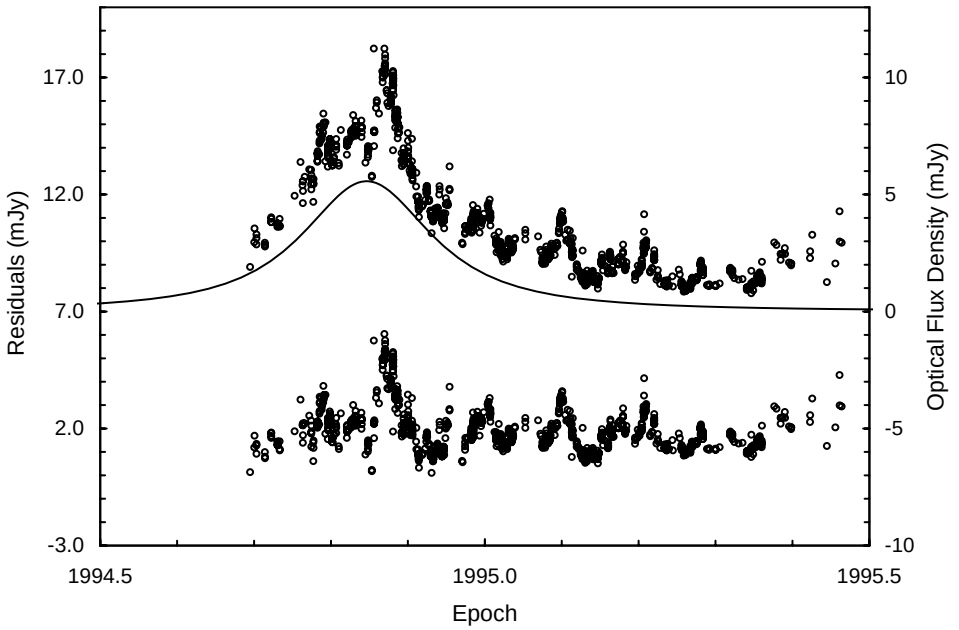

Fig. 4. Normalized boostimg factor δ^3 as a function of time in the observers reference frame (solid line), together with the observed V band flux density (upper points) and residuals (lower points), after substraction of the boosted intensity of the undelying jet

2.2. Boosting at optical wavelengths

Since we found satisfactory models for $\gamma > 6$, the final specification of this parameter was based on the behavior of the optical light curve during the periodic flares. In fact, the increase in δ as the jet approaches the line of sight produces boosting of the radiation in the optically thin part of the spectrum, being the possible cause of the periodic optical flares. The observed intensity has a dependence on the Doppler factor of the form $\delta^{3+\alpha}$ for a discrete feature and $\delta^{2+\alpha}$ for a continuous jet. Measurements of the spectral index α ($S_\nu \propto \nu^{-\alpha}$) in the optical part of the spectrum showed $\alpha \approx 1.5$ at epochs of minimum intensity (Kidger et al. 1991) and $\alpha \approx 1.0$ during the small bursts (Hagen-Thorn 1980). Since we do not have direct evidence of its value for the underlying jet, we fixed it for each model in such a way that the half-width of the function $\delta^{2+\alpha}$, with $\alpha > 0$ coincides with the value observed in the periodic optical flares. We found solutions only for $7 < \gamma < 8$, and the corresponding values of $1 > \alpha > 0$. Values of γ larger than 8 result in a very short half-life, even for $\alpha = 0$, and values of γ smaller than 7 require extremely high values of α.

Fig. 4 shows the behavior of the normalized function $\delta^{2+\alpha}$, for $\gamma = 7$ and $\alpha = 1$, together with the light curve for the 1994.85 flare obtained from the data arquive kept at Tuorla Observatory. The behavior of the residuals representing the difference between the observed V band flux density (in mJy) and the normalized function $\delta^{2+\alpha}$, shown in the lower part of the graph, is typical of the light curve before the flare (see Fig. 1 of Sillanpää et al. 1996).

In the model, the ratio between the maximum and minimum values of the Doppler factor is 12, therefore the jet emission is boosted by a factor 1700. Considering that the maximum flux density at the V band during the flare was 5 mJy above the quiescent value, the non-boosted flux density between flares would be 3 μJy. This value is much smaller than the measured optical emission, indicating that the underlying jet would not be visible at optical wavelengths except when boosted.

2.3. Boosting at radio frequencies

We will investigate the behavior of the flux density at radio frequencies. Let us assume that the turnover frequency between optically thin and thick emission, in the underlying jet spectrum, occurs at relatively low frequencies, like 37 GHz. We selected this frequency because there is available data, during and after the optical flare (Pietilä et al. 1999). In the quiescent phase, the flux density, obtained by extrapolating the expected optical emission, with spectral index $\alpha = 1$, would be 50 mJy, which is below the observed radio emission. Boosting will increase the contribution of the jet to the total radio flux density by a factor $\delta^{2+\alpha} \propto (12)^{1/2} = 3.5$, where we have used $\alpha = -1.5$ for the optically thick spectral index of a continuous jet. Therefore, even with boosting, the contribution of the jet to the total emission will be small, explaining the absence of a radio outburst associated to the optical flare.

It still remains to be verified why component K3, formed during the 1983 flare, and the features seen by Marscher & Marchenko (1997) during the 1994 flare do not present signals of boosting, even though, contrary to the jet emission, the shocked components are optically thin at radio frequencies. The explanation lies in the evolutionary nature of these features. If they are formed by shocks propagating along the jet, they will evolve through the well-known Compton, radiative and adiabatic phases, becoming optically thin at lower frequencies (e.g. Marscher 1990). In the latter phase, the intensity of the maximum in the spectrum varies as

$$S_{\rm m}(\nu_{\rm m}) \propto {\nu_{\rm m}}^{-\alpha_{\rm th}} \tag{10}$$

where $\alpha_{\rm th}$ is the spectral index of the optically thick part of the spectrum. Since the flux density is always smaller than $S_{\rm m}(\nu_{\rm m})$

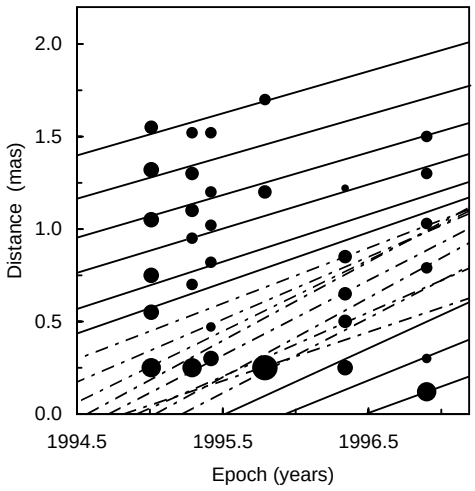

Fig. 5. Distance of superluminal features to the core as a function of time. Points represent the components found by Marscher & Marchenko (1997). Their size is proportional to the measured flux density. The lines represent possible trajectories, spaced by 17° in phase angle of the precessing jet obtained from the model with $\gamma = 7$. Solid lines correspond to epochs in which the jet is not very close to the line of sight, traced lines show the trajectories when the viewing angle is very small

and the frequency of the maximum in the comoving reference frame is a factor of δ smaller than the observed frequency, we have to introduce an additional factor $\delta^{\alpha_{th}}$ in the observed luminosity. The beamed radiation, in the optically thin part of the jet spectrum, is therefore given by:

$$S(\phi) \propto \delta^{2+\alpha}\delta^{\alpha_{\rm th}} \tag{11}$$

and the boosting is strongly reduced in accordance with the observations.

2.4. Superluminal features at the epoch of the 1995 flare

In this section we compare the positions of the superluminal features found by Marscher & Marchenko (1997) at several closely spaced epochs near the 1994 optical flare with possible trajectories predicted by our model. The identification of the components in the different maps was ambiguous and, depending on the choice, the velocities reported by Marscher & Marchenko varied between 6 and 8c (for $h = 1$ and $q_0 = 0.5$). In Fig. 5 we show several trajectories, derived from the model, superimposed to the features obtained from the VLBI maps. The trajectories correspond to the motion of features formed at equally spaced phase angles in the precessing jet.

The phase difference (17.1°) was chosen in such a way that the trajectories fitted the VLBI positions for the oldest and newest components. This phase difference corresponds to about one year interval for the formation of new superluminal components in the observer reference frame and agrees with the periodicity found by Hughes et al. (1998). The agreement between the observed features and the prediction of the model (full lines in the graph) is very good for the 5 features furthest from the core in the first three epochs and for the 3 features closest to the core in the last three epochs. Between these two sets, nine other trajectories, shown as broken lines, correspond to the same phase interval in the frame fixed at the source. Their proximity reflects the rapid change in the Doppler factor, which decreases the time scale in the observer reference frame and also changes the observed superluminal velocities. Therefore, a large number of features could have been formed in a small time interval. In fact, Marscher & Marchenko (1997) pointed out that the maps for the first three epochs showed well defined discrete features, while the maps from the last three epochs after the flare, presented a continuous distribution in flux density between 0.5 and 1.5 mas from the core. Also, we expect the evolution of these features to be faster, making difficult to identify them, even in closely spaced epochs. As in Marscher & Marchenko (1997), the size of the points in Fig. 5 is proportional to the observed flux density. The large intensity of the 0.2 mas feature in the Oct 1995 map could be the consequence of the superposition of the features in four very close trajectories, originated in 1994.82, 1994.92, 1995.04 and 1995.23 respectively. This superposition, together with the predicted formation of a new feature in 1995.52, confirmed by an increase in the core intensity, would appear as a second radio and optical flare. In fact, a second flare was seen almost a year after the 1972, 1983 and 1994 flares. Although the intensities of the two consecutive flares in 1994-1995 were similar, their origin is probably different. The first one has no correlation with radio emission, because it was originated in the underlying jet, optically thick at radio frequencies. The second flare was a consequence of the superposition of several superluminal features, and therefore, correlated to radio flares.

2.5. The high degree of polarization of the superluminal component K2

We will analyse the possible values of the degree of polarization of component K2, taking into account the viewing angle of the jet, predicted by our model for the epoch at which this component was formed, and compare them with the value of 64% measured by Roberts et al. (1987).

The degree of polarization of a partially compressed source of synchrotron radiation is given by (Hughes et al. 1985):

$$m \approx \frac{2\alpha+2}{2\alpha+10/3} \times \frac{1-k^2\cos^2\epsilon}{2-(1-k^2)\cos^2\epsilon} \tag{12}$$

where α is the spectral index of the optically thin synchrotron radiation, k the amount of compression and ϵ the angle between the plane of compression and the line of sight in the frame of the emitting material. This angle is related to the angle ϕ between the jet and the line of sight by the aberration formula:

$$\cos\phi = \frac{\sin\epsilon + \beta}{1+\beta\sin\epsilon} \tag{13}$$

Combining this expression with Eq. (5) we obtain:

$$\beta_{\rm obs} = \beta\gamma\cos\epsilon \tag{14}$$

For our component K2 $\beta_{\rm obs} = 3.7 \pm 0.6$ for $h = 0.7$, using $\gamma = 7$ from the precessing model, we obtain $\epsilon = 32^\circ \pm 6^\circ$. For this angle, there is no value of k for which 64% linear polarization could be obtained.

Cawthorne & Wardle (1988) calculated the degree of polarization when the shock velocity is different from the jet bulk velocity. They found:

$$\beta_{\rm obs} = \beta\gamma\cos\phi_{\rm s} \tag{15}$$

and

$$\frac{\sin^2\phi_{\rm s}(1-{\beta_{\rm d}}^2)}{(1+\beta_{\rm d}\cos^2\phi_{\rm s})^2} = \frac{2m/m_0}{1+m/m_0} \times \frac{(1-{\beta_{\rm d}}^2)}{(1-9{\beta_{\rm d}}^4)} \tag{16}$$

where $m_0 = (2\alpha+2)/(2\alpha+10/3)$, $\phi_{\rm s}$ is the angle between the jet and the line of sight in the rest frame of the shock and $\beta_{\rm d}$ the speed of the emitting material after the passage of the shock.

From Eqs. (15) and (16) we obtain $\phi_{\rm s} = 32^\circ \pm 6^\circ$ and $\beta_{\rm d} \approx 1/3$, the minimum value allowed for the upstream velocity when an extreme relativistic equation of state is used (Cawthorne & Wardle 1988). The Doppler factor that produces the beaming can be written as:

$$\delta = \delta_{\rm s}\delta_{\rm fs} = [\gamma(1-\beta\cos\phi)]^{-1}[\gamma_{\rm d}(1-\beta_{\rm d}\cos\phi_{\rm s})]^{-1} \tag{17}$$

where $\delta_{\rm s}$ and $\delta_{\rm fs}$ are respectively, the Doppler factors of the shock in the observer frame and of the fluid in the shock frame. The value of $\delta_{\rm fs}$ is in our case 1.10 ± 0.02 and therefore, $\delta \approx \delta_{\rm s}$ does not affect our determination of the Lorentz factor γ from the width of the optical light curve.

3. Discussion

The periodic light curve of OJ287 was explained by the beaming of the optically thin radiation originating in a relativistic precessing jet as it approaches the line of sight. The work of Katz (1997) demonstrated the possibility of having precession periods of only a few years in a binary black hole system when the accretion disk of the primary does not coincide with the orbital plane. Pairs of black holes can be formed as a consequence of interactions and eventually merging of galaxies. The difference in position between the BL Lac object OJ287 and the center of the faint underlying nebulosity could be considered as observational evidence of this merging phenomena (Heidt et al. 1999).

A moderate value of γ was found for the jet, in contrast to the value of 20 estimated by Katz (1997). The discrepancy is due to a misinterpretation of the relation between the duration of the periodic optical flares and the orbital phase, since it was not taken into account the fact that the precession velocity is not constant in the observer reference frame (Abraham & Carrara 1997).

The projected angle η of the jet in the plane of the sky vary between -65° and -178°. The kpc scale jet is initialy directed along $\eta = -90^\circ$ (Perlman & Stocke 1994), well within the allowed jet directions. Gabuzda & Cawthorne (1996) found two new features (K4 and K5) in the VLBI map of OJ287 for epoch 1990.47. Their position angles are compatible with the precessing jet model, allowing for the uncertainties introduced by the poor coverage of the uv plane in the north south direction. The predicted velocity would be $\beta_{obs} \approx 2.6h^{-1}$, not very different from the velocities of the other features. K5 can be identified with feature A in the 43 GHz map at epoch 1991.27 (Tateyama et al. 1996) and in the maps of Marscher & Marchenko (1997) as the features furthest from the core in the first four maps.

Close to the epoch of the 1994 flare, it was found a periodicity in the formation of superluminal features of about one year in the reference frame center at the source, which corresponds to about 17° in the precessing jet phase. The superposition of closely spaced trajectories at the epoch of maximum approach to the line of sight can account for the second flare, observed both at radio and optical wavelengths, about one year after the periodic flares.

The superluminal features found by Tateyama et al. (1999) in the analysis of Geodetic VLBI data at 8.3 GHz have velocities larger than those found by Gabuzda & Cawthorne (1996) at earlier epoch, which were used in the fitting of our model. We belive that the discrepancy is due to the small number of components allowed in the model fitting and the incomplete coverage of the time series in the Geodetic data.

The angle between the jet and the line of sight varies between 2.6° and 28.2°, the corresponding Doppler factors, for $h = 0.7$ are, respectively, 12.8 (during the outbursts) and 1.1 (most of the time). Madejski & Schwartz (1983) calculated the beaming factor δ from the ratio of the measured X-ray fluxes and those expected from the synchrotron self-Compton process and obtained the values of 0.47 and 1.7, depending on the choice of the synchrotron self absorption frequency. Madau et al. (1987), on the other hand, reported a value of 8.7 using similar data, the difference being the choice of the geometrical parameters. Considering the large uncertainty in the values estimated for δ, the prediction of the precessing jet model seems reasonable, it accounts for boosting and fast variability during the strong flares and it can probably accommodate the observed X-ray emission when no beaming is present.

The model can also explain the high degree of polarization detected in component K2 by Roberts et al. (1987), if the shock moves with a speed $\beta_d = 0.33$ in the reference frame of the jet. The Doppler factor introduced by this velocity is very close to unity and does not affect the boosting properties of the model.

This work was partially supported by the Brazilian agencies FAPESP and CNPq. I would like to thank G. Romero for helpful discussions.

References

Abraham Z., Carrara E.A. 1998, ApJ 496, 172
Abraham Z., Romero G.R. 1999, A&A 344, 61
Aller H.D., Hughes P.A., Aller M.F. 1991, In: Miller H.R., Wiita P.J. (eds.) Variability of Active Galactic Nuclei, Cambridge Univ. Press, Cambridge, p. 172
Carrasco L., Dultzin-Hacya D., Cruz-Gonzalez I. 1985, Nature 314, 146

Cawthorne T.V., Wardle J.F.C. 1988, ApJ 332, 696
Comastri A., Molendi S., Ghisellini G. 1995, MNRAS 277,297
Gabuzda D.G., Wardle J.F.C., Roberts D.H. 1989, ApJ 336, L59
Gabuzda D.C., Cawthorne T.V. 1996, MNRAS 283, 759
González-Pérez J.N., Kidger M.R., de Diego J.A. 1996, A&A 311, 57
Hagen-Thorn V.A. 1980, Ap&SS 73, 263
Heidt J., Nilsson K., Appenzeller I., et al., 1999, A&A 352, L11
Hughes P.A., Aller H.D., Aller M.F. 1985, ApJ 298, 301
Hughes P.A., Aller H.D., Aller M.F. 1998, ApJ 503, 662
Jannuzi B.T., Yanni B., Impey C. 1997, ApJ 491, 146
Katz J.L. 1997, ApJ 478, 527
Kidger M.R., Takalo L.O., Valtaoja E., et al., 1991, A&A 252, 538
Kollgaard R.I., Wardle J.F.C., Roberts D.H., et al., 1992, AJ 104, 1687
Lehto H.J., Valtonen M.J. 1996, ApJ 460, 207
Madau P., Ghisellini G., Persic M. 1987, MNRAS 224,257
Madejski G.M., Schwartz D.A. 1983, ApJ 275, 467
Marscher A.P., 1990, In: Zensus A.J., Pearson T.J.(eds.), Superluminal Radio Sources, Cambridge University Press, 280
Marscher A.P., Marchenko S.G. 1997, In: Tosti G., Takalo, L. (eds.) Multifrequency Monitoring of Blazars, Publ. Astron. Univ. di Perugia, p. 68
Pietilä H., Takalo L.O., Tosti G., et al., 1999, A&A 345, 760
Perlman E.S., Stocke J.T. 1994, AJ, 108, 56
Roberts D.H., Gabuzda D.C., Wardle J.F.C. 1987, ApJ 323, 536
Schrader C.R., Hartman R.C., Webb J.R. 1996, A&AS 120, 599
Sillanpää A., Teerikorpi P., Haarala S., et al., 1985, A&A 147, 67
Sillanpää A., Haarala S., Valtonen M.J., et al., 1988, ApJ 325, 628
Sillanpää A. 1991, A&A 247, 11
Sillanpää A., Takalo L.O., Nilsson K., et al., 1999, In: Takalo L.O., Sillanpää A. (eds.) BL Lac Phenomenon, ASPS, p. 395
Sillanpää A., Takalo L.O., Kikuchi S., Kidger M., De Diego J.A., 1991, AJ 101, 2017
Sillanpää A., Takalo L.O., Pursino T., et al., 1996, A&A L17
Smith P.S., Balonek T.J., Elston R., et al., 1987, ApJS 64, 459
Tateyama C.E., Inoue M., Krichbaum T. P., et al., 1996, PASJ 48, 37
Tateyama C.E., Kinghann K.A., Kaufmann P., et al., 1999, ApJ 520, 627
Urry C.M., Sambruna R.M., Worrall D.M., et al., 1996, ApJ 463, 424
Valtaoja E. 1996, In: Miller H.R., Webb J.R., Noble J.C. (eds.) Blazar Continuum Variability,
Vicente L., Charlot P., Sol H. 1996, A&A 312, 727 (San Francisco: Astron. Soc. of the Pacific), p. 226
Worral D.M., Puschell J.J., Jones B., et al., 1982, ApJ 261, 403